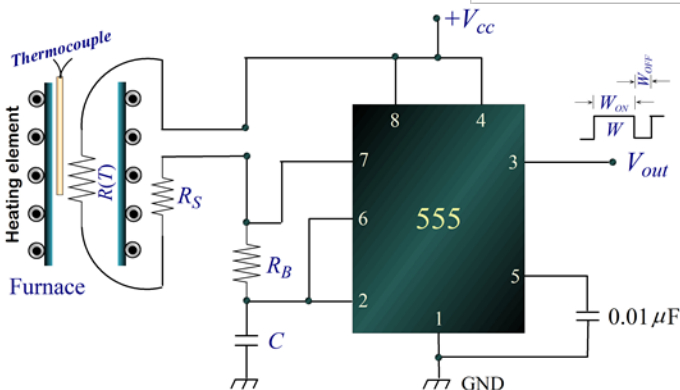
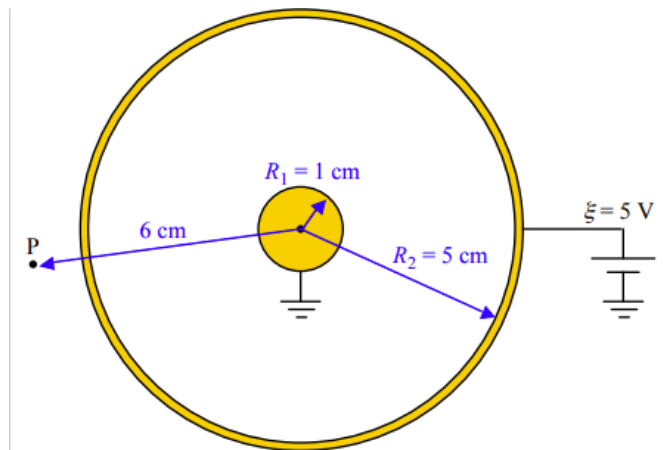
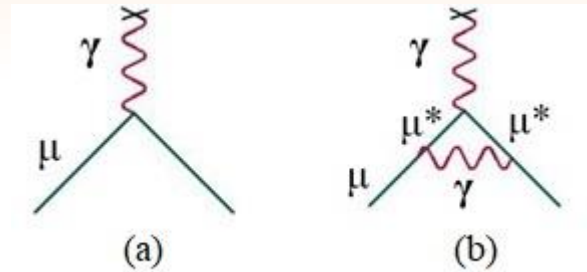


ISSN 0970-5953

Volume 37. No. 1

January - March 2021

PHYSICS EDUCATION



www.physedu.in

Volume 37, Number 1**In this Issue**

- ❖ Hidden Physics of Muon $g-2$** 07 Pages
Nitali Dash and Manasi Goswami
- ❖ Introducing of delta function in generalized space and their application in quantum mechanics** 08 Pages
Samkhaniani, Saba and Jafari Matchkolaee Mehdi
- ❖ Solutions for simple quantum mechanical systems using SCILAB** 09 Pages
Pankaj A. Nagpure
- ❖ A simple model of electric ground and of a dc power supply** 05 Pages
Carl E. Mungan
- ❖ Realizing Positive Temperature Co-efficient of Resistance Effect using an IC-555 Timer Circuit** 05 Pages
K. M. Anand, J. Mukherjee and K. Prasad

Hidden Physics of Muon $g - 2$

Nitali Dash and Manasi Goswami

DESM (Physics), Regional Institute of Education (NCERT),
Bhubaneswar 751022, India.

nitali.dash@gmail.com ; manasigoswami62@gmail.com

Submitted on 27-05-2021

Abstract

The recent results of muon $g - 2$ experiment conducted at Fermilab, USA has created a sensation in the field of particle physics. The gyromagnetic ratio 'g' of muon found from muon $g - 2$ experiments differ from the Standard Model expectation value of 2. This paper explores the significance of muon and compares the results obtained from various muon $g - 2$ experiments conducted at different laboratories across the World. The prospects of muon and the underlying hints of muon anomaly to explore the physics beyond the Standard Model has also been highlighted.

1 Introduction

Muon, a heavier relative of the electron is a point-like particle. Unlike proton it has no composite parts, so the properties of the muon is all it's own. Muon is 207 times heavier than an electron, which makes it more sensitive to new types of virtual particles [1]. A muon has intrinsic magnetic

property. Moreover, like a spinning top, it also has an angular momentum, called spin. Therefore muons gyromagnetic ratio 'g' is determined by its magnetic strength and rate of its magnetic gyration. The muon $g - 2$ experiment has been assigned such a name basing on the fact that the gyromagnetic ratio 'g' of muon differs from the Standard Model expected value of 2. This anomaly is called the anomalous magnetic moment of the muon and this anomaly is now challenging the Standard Model of physics. In a recent experiment of muon $g - 2$ conducted at Fermilab, USA, scientists have found that this subatomic particle muon is disobeying the highly accepted theories of particle physics prescribed in the Standard Model. The Standard Model developed in 1970, is the widely accepted mathematical explanation for the known and predicted behavior of all the particles of the Universe. The significant disagreement between the particle's newly measured behavior and the Standard Model appropriate behavior hints that the Universe may contain unseen particles

and forces beyond the purview of the Standard Model. The recent experimental results from various laboratories across the globe have also provided enough evidence that this tiny subatomic particle, muon seems to be disobeying the known laws of physics. Muon $g - 2$ is a particle physics experiment conducted at Fermilab, USA to measure the anomalous magnetic dipole moment of a muon to a precision of 0.14 parts per million. The experimenters believe that muon $g - 2$ anomalies will better understand the properties of muon and use them to probe the future prospect of the Standard Model physics.

In this article, we review the significance of muon and its magnetic moment anomaly that may lead to physics beyond the Standard Model and its prospect.

2 Significance of Muon

Like all other planets in the Universe, every moment Earth is hit by enormous number of very high energy particles and nuclei originating from astrophysical sources called primary cosmic rays [2]. Further the interaction of these primary cosmic rays with Earth atmosphere (15 km) creates a shower of many other particles. The shower of these particles especially includes electron-positron (e^+e^-) pairs, muons (μ^\pm) and neutrinos ($\bar{\nu}_\mu, \nu_\mu$). The neutral pi-mesons (π^0) decay to photons (γ), which further create e^+e^- pairs. However, the decay chain of charged mesons (π^\pm) produces μ^\pm and

$\nu_\mu(\bar{\nu}_\mu)$ as shown in Eq[1].

$$\pi^\pm \rightarrow \mu^\pm + \nu_\mu(\bar{\nu}_\mu) \quad (1)$$

The discovery of muons had taken place in 1930s by the working group of Anderson and Neddermeyer while observing a photograph of a highly penetrating track of minimum ionized particle in the cloud chamber from cosmic ray. Like electrons, the positive charge of muon represents its antiparticle and there are no neutral muons. Muons can also be produced artificially in high energy collisions at an accelerator using the same channel. Positive and negative muons have the same rest mass of $106 \text{ MeV}/c^2$ and the same spin of $1/2$. Both decay with a relatively long mean life of $2.2 \mu\text{s}$ into electrons and neutrino-antineutrino pairs as given in Eq[2]. The long mean lifetime of muon allows scientists to make precision measurements of its properties before it decays to respective particles and anti-particles.

$$\mu^\pm \rightarrow e^\pm + \bar{\nu}_\mu(\nu_\mu) + \nu_e(\bar{\nu}_e) \quad (2)$$

Because of their relatively slow lifetime, they can reach the Earth's surface with speed of light. Before reaching the ground, they roughly lose about 2 GeV energy to ionization while traveling through the Earth atmosphere. Thus, they are the most numerous charged particles of cosmic ray found at sea level. The energy loss and decay of muon ultimately reflects its energy and angular distribution spectrum at the sea level. So, the mean energy of the muons at the ground or sea level is $\sim 4 \text{ GeV}$.

3 Magnetic Moment Anomaly

Analogous to classical mechanics in quantum mechanics, the intrinsic spin angular momentum (\vec{S}) of an elementary charged particle produces magnetic dipole moment ($\vec{\mu}$) as expressed in Eq[3].

$$\vec{\mu} = g \frac{q}{2m} \vec{S} \quad (3)$$

Where, $q = \pm e$ is the charge of the particle in terms of the magnitude of the electron charge e , m is the mass of the charged particle, and the proportionality constant g is the gyromagnetic ratio also called g -factor. Stern-Gerlach in 1921 while studying atomic and sub-atomic magnetic moments of silver atom, and in 1927 Phipps and Taylor while studying hydrogen atom, the g -factor of the electron was found to be 2. The factor of 2 was obtained from the experimental observation of a two-band structure of the sample atoms with a separation of one Bohr magneton ($\mu_B = \frac{e\hbar}{2m_e}$) which is due to the unpaired spin of an atomic electron. However, the Diracs (1927) relativistic wave equation for electron is also in good agreement with its experimentally observed g value. Despite the success of the Dirac equation, the discrepancies with Dirac theory was accounted for by introducing a radiative correction term by Schwinger in 1947 while explaining hyperfine structure in hydrogen atom. This radiative correction (Figure 1(b)) term is called one-loop (lowest order) correction to $g_\mu^{SM} = 2$ (Figure 1(a)). This radiative correction term is also true for electron sibling i.e muon (μ) resulting in g -factor

(g_μ) greater than 2.

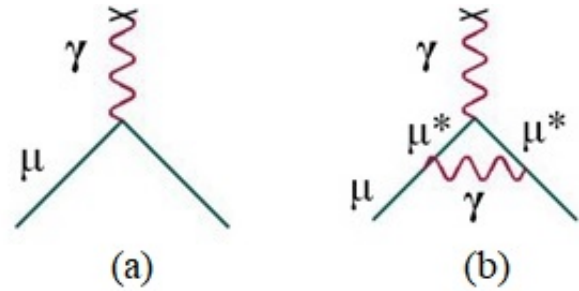


Figure 1: The Feynman diagrams for: (a) $g_\mu^{SM} = 2$; (b) The lowest order radiative correction.

So theoretically, the general expression for muon magnetic moment [3] can be written as,

$$\mu = (1 + a_\mu) \frac{q\hbar}{2m} , \quad (4)$$

where, $a_\mu = \frac{g_\mu - 2}{2}$ is a dimensionless quantity and is referred as the anomaly. The corresponding magnetic moment is called anomalous magnetic moment. As the experiments are measuring muon g -factor which deviates from 2, hence their name is muon $g - 2$ experiments.

4 Muon $g - 2$ Experimental Results

The kinematics of muon decay is central to the measurement of muon anomaly [4]. Because of parity violation in weak interaction, the decay of charged pions produce longitudinally polarized muons. When muons are injected into the uniform magnetic field, the decay electron/positron provides the muon spin direction. By measuring the muon

cyclotron frequency and the spin precession frequency, the anomalous angular frequency can be obtained from which anomalous magnetic moment (a_μ) can be determined. The precision in the measurements in the muon anomaly from successive experiments conducted at various laboratories across the World are listed below. In 1960, the Columbia University was the first to measure the muon magnetic moment with a precision of about 5% showing the same value of 'g' as that of electron [5].

4.1 Muon $g - 2$ Experiment at CERN

The muon $g - 2$ experiments began at CERN using cyclotron in 1959, and the first result was published in 1961 with 2% precision and the next result was published with 0.4% precision. In 1966 using Proton-Synchrotron, the result showed a quantitative discrepancy between the experimental and the theoretical values of a_μ with 25 times more precise than the previous ones. To avoid the systematic difficulties of the existing experiment, the third muon storage ring [6] experiment at CERN (1969 - 1976), confirmed the theory with a precision of 0.0007% [6] at a particular energy called magic energy i.e. 3.1 GeV [6]. The storage ring uses electric quadrupoles for vertical focusing of the beam. The electric field due to these electric quadrupoles creates motional magnetic field in the rest frame of muon. This motional magnetic field affect the spin precession frequency and hence the anomalous angular frequency of muon. This

additional contribution to anomalous angular frequency vanishes at a particular energy called magic energy. Moreover, at magic energy the anomalous angular frequency of muon depends only on applied magnetic field. Hence it becomes easy to estimate the anomalous angular frequency of muon [6].

4.2 Muon $g - 2$ Experiment at BNL

After 20 years later, the muon storage ring experiment at Brookhaven National Laboratory (BNL) [7] achieved a new standard in precision at the same magic energy of 3.1 GeV. It had used the same measurement principle as CERN but with a very high-intensity beam and directly injecting muons to the storage ring instead of pions. The experiment took data with positive and negative muons separately between 1997 to 2001. The final result obtained was in accordance with similar precision from positive and negative muons data, which were found to be inconsistent with the Standard Model theory contributing to new physics.

4.3 Muon $g - 2$ Experiment at FNAL

The muon $g - 2$ experiments at Fermi National Accelerator Laboratory (FNAL) [8] measured a_μ using the same muon storage ring as used at BNL but with improved magnetic field intrinsic uniformity. It also used a similar concept as executed in BNL for the anomaly measurement. The FNAL result is found to be in excellent agreement with the previous BNL measurement only with 3.3

standard deviations greater than the Standard Model prediction. The estimated value

of a_μ in Standard Model is $1659181.0 \pm 4.3 \times 10^{-10}$ [9].

The results of a_μ obtained from above mentioned experiments are listed in table below. The error in the results includes quadrature combination of systematic, statistical and fundamental constant uncertainties.

Experiment	Years	a_μ	Reference
CERN	1979	$1165924 \pm 8.5 \times 10^{-9}$	[6]
BNL Average	1999, 2000, 2001	$11659208.0 \pm 6.3 \times 10^{-10}$	[7]
FNAL	2021	$11659204.0 \pm 5.4 \times 10^{-10}$	[8]
BNL, FNAL	2021	$11659206.1 \pm 4.1 \times 10^{-10}$	[8]

5 Future Scope

The recent result of muon $g - 2$ is quite exciting and possibly hints towards the explanation of quires that the Standard Model has lacked behind. Generally, antimatter is created by radioactive decay and is also produced by cosmic rays and lightning. But within a very short duration, the produced antimatter bounce into matter resulting in more matter than antimatter in the Universe. Similarly, dark matter has not been explained by the Standard Model as it does not interact electromagnetically but constitute the crucial part of the origin of the Universe. The muon magnetic anomaly is not only sensitive to all four fundamental interactions of the Standard Model but also can reveal a new type of fundamental interaction. So the anomaly may explain this new type of interaction which may

exist beyond the Standard Model, matter-antimatter asymmetry, and the possible existence of dark matter in the Universe, etc.

Apart from the above-mentioned facts during last few decades the amazing muon has been used as a tool for betterment of science and society because of the advanced technology deployed in nuclear and particle physics [10]. At first, they were used in the 1960s to take X-ray photography of Chephrens pyramid to investigate hidden and unknown chambers, by the method of absorption of muons (attenuation of the cosmic-ray flux) while passing through it. Muons have also been used to probe the geological structure of the volcano, Mt. Asama, Japan in 2004 and confirmed the complete meltdown of the Japanese Fukushima reactor in the 2011 disaster. Using cosmic-ray muons, now-a-days with more developed detectors and tech-

niques have opened up the possibility to image precisely very large volume containers, cargo vehicles, train stations, etc. to detect any explosive materials (bombs, fissile material).

Muons are being used to study the properties of new compound materials that have the potential to provide novel semiconductors for the electronics industry or room-temperature superconductors and also has capability to observe the phenomena of “magnetricity” in “spin-ice” (i.e. magnetic version of electronics). This technique was first used at the UK ISIS facility using accelerator generated muons.

6 Summary

The Universe is the embodiment of particles. The observed behavior of the particles is governed by certain forces. To understand, describe and predict the nature and behavior of all the particles of the Universe physicists have framed a model called Standard Model. This model has been developed taking into account all particles and forces discovered so far. The Standard Model is a valid model which successfully describes the observed and predicted behaviors of all known particles of the Universe. However, disagreement of observed results from the predicted results of the Standard Model raises two pertinent questions :

- Is Standard Model theory is valid Universally?

- Are there new, as yet unobserved particles and forces that exist in nature?

A popularly addressed muon $g - 2$ experiment recently conducted at Fermilab, USA, with highest precision has created a new sensation in the world of particle physics. It has been confirmed from the experiment that the gyromagnetic ratio g of the muon differs from the simple expectation of 2. Hence, this disagreement has opened up many possibilities and many questions also. Muon $g - 2$ sensation may create a new theory in the near future.

References

- [1] <https://muon-g-2.fnal.gov/the-physics-of-g-2.html>
- [2] M. Tanabashi et al., Phys. Rev. D98 no. 3, 030001 (2018).
- [3] J. P. Miller et al., Ann. Rev. Nucl. Part. Sci. 62, 237 (2012).
- [4] F. Jegerlehner and A. Nyffeler, Phys. Rept. 477, 1 (2009).
- [5] R. L. Garwin et al., Phys. Rev. 118, 271 (1960).
- [6] J. Bailey, et al. (CERN-Mainz-Daresbury Collaboration), Nucl. Phys. B150, 1 (1979).
- [7] G. W. Bennett et al. (Muon $g - 2$ Collaboration), Phys. Rev. D73, 072003 (2006).

- [8] B. Abi et al. (Muon $g - 2$ Collaboration), Phys. Rev. Lett. 126, 141801 (2021).
- [9] T. Aoyama et al., Phys. Rept. 887, 1 (2020).
- [10] G. Bonomi et al., Nucl. Phys. 112, 103768 (2020).

Introducing of delta function in generalized space and their application in quantum mechanics

Samkhaniani, Saba ¹ and Jafari Matehkolae, Mehdi ²

¹Department of Engineering, Alzahra University
Tehran, Iran.

²Faculty of Physics, Semnan University
Semnan, 35131-19111, Iran.

mehdijafarimatehkolae@gmail.com

Submitted on 16-12-2020

Abstract

This paper shows that the delta function can be displayed independently in a generalized space. We show why the delta function is important in a generalized space. In this regard, we review the essential properties of the delta function on the smooth manifold. Then, we deduce the Heisenberg canonical computational relation and a universal formula for the adjoint of a linear operator on the smooth manifold by using the definition of delta function in generalized space.

1. Introduction

Delta function has been introduced by Dirac in his renowned book [1] as a function which has some very unusual properties. This function is so familiar

for physicists and it has so many applications in different areas of physics and mathematics. There are many reports about this function that are usually associated with its applications in different branches of physics. Some of these applications include a unified representation of the distribution of a function of one or several random variables. It is also applied to model an impulse and other distributions such as a point charge, point mass or electric point. In quantum mechanics, for instance, by using delta function, the canonical commutation relation has been investigated between the momentum and position operators and the Ehrenfest theorem was derived for the free particle. Dirac delta function is one of the examples given for the zeroth theorem of the history of science [2]. There is a

pedagogical paper that illustrates the application of delta function in quantum mechanics through different examples [3]. This function in the form of potential function has been studied many times in non-relativistic quantum mechanics [4-9]. For a useful text to review Delta function in details, see [10].

Some of the most important properties of delta function, which usually exists in the textbooks, are as follows:

$$\int_{-\infty}^{\infty} f(x)\delta(x)dx = f(0) \tag{1}$$

where $\delta(x)$ is the delta function and $f(x)$ is a test function that should be continuous. If the $f(x)$ is discontinuous at $x=0$, there is an impressive and good discussion [11]. From (1), we can conclude

$$x\delta(x) = 0 \tag{2}$$

One can obtain two results from the above statement. Firstly, the associative law does not hold for delta function. In this case, there is a usual example [12, 13]:

$$\left(\frac{1}{x}\right)x\delta(x) = 1.\delta(x) = \delta(x) \tag{3}$$

$$\frac{1}{x}.(x\delta(x)) = \frac{1}{x}.0 = 0 \tag{4}$$

Secondly, we may add any finite multiple of this zero (2) to one side of an equation

$$A(x) = B(x) = B(x) + cx\delta(x) \tag{5}$$

where c is an arbitrary finite constant. However, if we should divide both sides by x , the addition $c\delta(x)$ is no longer zero at $x=0$. Hence

$$\frac{A(x)}{x} = \frac{B(x)}{x} + c\delta(x) \tag{6}$$

Which is not necessarily true for any arbitrary value of c . As an example for the above equation we can write

$$\frac{d}{dx} \ln x = \frac{1}{x} + c\delta(x) \tag{7}$$

where $c = i(2n+1)\pi$ and n is any integer.

$$\frac{A(x)}{x} = \frac{B(x)}{x} + i(2n+1)\pi\delta(x) \tag{8}$$

One of the most important properties of delta function is

$$\delta(g(x)) = \sum_a \frac{\delta(x-a)}{|g'(a)|} \tag{9}$$

where $g(a) = 0$ and $g'(a) \neq 0$ [14]. This equation plays crucial role in the section 5 of our paper. In general, our idea of the generalized delta function is related to employing a generalized space to define delta function.

In section 2 we try to answer the original question: why the representation of delta function in generalized space is important? In section 3 we introduce generalized delta function and its

fundamental properties in generalized space. In section 4, we endeavor to deduce the Heisenberg commutation relation by using generalized delta function; it is worthwhile that we don't use the representation of the momentum operator in generalized space. Finally, in section 5, we show that one of the applications of generalized delta function is computing a universal formula for the adjoint of a linear operator in Hilbert space.

2. Why generalized delta function is important?

The "relativity revolution" and the "quantum revolution" are among the greatest successes of twentieth-century physics, yet the theories they produced appear to be fundamentally incompatible. General relativity remains a purely classical theory and describes the geometry of space and time as smooth and continuous, whereas quantum mechanics is related to microscopic world. Many attempts have been made to unify two theories, and one of the ideas to the unification of these theories is quantized gravity [15-19].

Just as the orthonormality condition for two vectors in continuum space is the Dirac delta function, we need to display this function in generalized space to represent Hilbert space. Therefore, generally for the representation of quantum mechanics in generalized space, it is necessary to know the form of the delta function.

For example, to deduce momentum operators in generalized space one can use generalized delta function. In the renowned paper [20], directly and according to the generalized delta function, the momentum operator has been represented.

Now, there are different approaches to represent the momentum operators in generalized space [20-27]. The form of the momentum operators in generalized space is as follows:

$$P_i = -i\hbar \left(\frac{\partial}{\partial x^i} + \frac{1}{2} \Gamma_{ji}^j \right) = -i\hbar \frac{1}{\sqrt[4]{g}} \frac{\partial}{\partial x^i} \sqrt[4]{g} \quad (10)$$

where $\Gamma_{ji}^j(x) = \frac{\partial}{\partial x^i} \ln(\sqrt{g(x)})$. where Γ_{ji}^j is the Christoffel symbol and is defined by $\Gamma_{ji}^j(x) = \frac{\partial}{\partial x^i} \ln(\sqrt{g(x)})$.

Also, recently the representation of the inverse momentum operator in generalized space has been obtained [28].

3. Generalized delta functions

Suppose a manifold with an atlas consisting of only one chart, equipped with the metric $g_{ij} : i, j = 1, 2, \dots, n$; n being the dimension of the manifold. The manifold is such that there exists a global one-to-one correspondence between the points of the manifold and \mathbb{R}^n . Therefore, we will work only within the system of the coordinates x^i defined on all \mathbb{R}^n representing the manifold. The

metric is $ds^2 = g_{ij}(x)dx^i dx^j$ where $g \equiv |\det g_{ij}|$.

From the reference [3], we define the normalized kets $|x\rangle$ in coordinate representation of the Hilbert space in generalized space so that

$$X^i |x\rangle \equiv |x\rangle x^i, \int d^n x \sqrt{g} |x\rangle \langle x| = 1 \quad (11)$$

In equation (11), X^i is an operator with real eigenvalues x^i . Note that, x^i are the coordinates that cover all \mathbb{R}^n .

At first we consider the normalized eigenvectors of position which satisfy

$$\langle x' | x'' \rangle = \delta(x', x'') \quad (12)$$

where $\delta(x', x'')$ is the generalized delta function [4]. We can define

$$\delta(x', x'') = 0 \text{ for } x' \neq x'' \quad (13)$$

And

$$\int \zeta(x') \delta(x', x'') h(x') = h(x'') \quad (14)$$

where ζ is the invariant volume element $\zeta(x') = g^{\frac{1}{2}}(x') d^n x'$, and g is the square root of the absolute value of the determinant of the metric matrix.

The relation between the delta function and the generalized delta function is as following

$$\delta(x', x'') = \frac{\delta(x' - x'')}{\sqrt{g(x')}} = \frac{\delta(x' - x'')}{\sqrt{g(x'')}} \quad (15)$$

Since we know that $(x'^i - x''^i) \delta(x', x'') = 0$ and

$$\frac{\partial}{\partial x'^j} (x'^i - x''^i) = \delta_j^i, \text{ then one can write}$$

$$(x'^i - x''^i) \frac{\partial}{\partial x'^j} \delta(x', x'') = -\delta_j^i \delta(x', x'') \quad (16)$$

From the basic point $f(x) \delta(x) = f(0) \delta(x)$ we have

$$f(x) \delta'(x) = f(0) \delta'(x) - f'(0) \delta(x) \quad (17)$$

Now, by using the equations (15) and (17) we obtain

$$\begin{aligned} \frac{\partial}{\partial x'^i} \delta(x', x'') = \\ \frac{1}{\sqrt{g(x')}} \frac{\partial}{\partial x'^i} \delta(x' - x'') - \frac{\delta(x' - x'')}{\sqrt{g(x')}} \frac{\partial}{\partial x'^i} \ln(\sqrt{g(x'')}) \end{aligned} \quad (18)$$

Again, with respect to the property of the ordinary delta function, that is

$$\frac{\partial}{\partial x''^i} \delta(x' - x'') = -\frac{\partial}{\partial x'^i} \delta(x' - x'')$$

we can differentiate the generalized delta function in different points:

$$\frac{\partial}{\partial x''^i} \delta(x', x'') = \frac{-1}{\sqrt{g(x'')}} \frac{\partial}{\partial x'^i} \delta(x' - x'') \quad (19)$$

After comparing equations (18) and (19) we obtain the final equation

$$\frac{\partial}{\partial x^i} \delta(x', x'') = -\frac{\partial}{\partial x''^i} \delta(x', x'') - \Gamma_{ji}^j \delta(x', x'') \quad (20)$$

Note that, Equation (20) can be used directly to calculate the momentum operator in a generalized space [20].

4. Heisenberg commutation relation

The canonical commutation relation has been investigated in ref. [29] between the momentum and position operators and the Ehrenfest theorem was derived for the free particle. The only assumption in this reference is the spatial uniformity of the probability density to find the particle. In any way, here we are looking for the representation of generalized delta function and its fundamental properties. We can show that the properties of a generalized delta function are very different from those of a Dirac delta function and that they behave like a pole in the complex plane.

Now, we can define the pure wave plane on the mentioned manifold

$$\langle x | p \rangle = \langle p | x \rangle^* = \frac{e^{ip \cdot x}}{(2\pi\hbar)^{\frac{n}{2}}} \quad (21)$$

And

$$\frac{1}{\sqrt{g(X)}} \int d^n p |p\rangle \langle p| = \int d^n p |p\rangle \langle p| \frac{1}{\sqrt{g(X)}} = 1 \quad (22)$$

Without the momentum operator representation in generalized space, we indicate the canonical relation between position and momentum operators.

According to the definition (11) and by using the equation (22) we can write

$$\begin{aligned} [X^i, P_j] &= X^i P_j - P_j X^i \\ &= \int d^n x d^n p (x^i p_j) |x\rangle \langle x| p\rangle \langle p| - \int d^n x d^n p (p_j x^i) |p\rangle \langle p| x\rangle \langle x| \end{aligned}$$

Now with respect to the equation (21) we can continue the procedure to find

$$\begin{aligned} &= \int d^n x d^n x' \frac{d^n p}{(2\pi\hbar)^{\frac{n}{2}}} \sqrt{g(x')} (x^i p_j) \left[e^{\frac{ip_j x'}{\hbar}} e^{-\frac{ip_j x^i}{\hbar}} |x\rangle \langle x'| - e^{\frac{ip_j x^i}{\hbar}} e^{-\frac{ip_j x'}{\hbar}} |x'\rangle \langle x| \right] \\ &= -i\hbar \int d^n x d^n x' x^i \left[|x\rangle \langle x'| \frac{\partial}{\partial x_j} \delta^n(x-x') - |x'\rangle \langle x| \frac{\partial}{\partial x_j} \delta^n(x'-x) \right] \\ &= i\hbar \delta_j^i \int d^n x \sqrt{g(x)} |x\rangle \langle x| = i\hbar \delta_j^i \quad (23) \end{aligned}$$

We have used equation (16) to derive the above result.

5. Application of generalized delta function

In this section we consider two explicit examples for generalized delta function. One of them is the application of the equation (20). Indeed, this equation is used directly to obtain the momentum representation in the generalized space as it seen in ref. [20], in detail.

For other example, same of the ref. [31], we can obtain a universal formula for the adjoint of arbitrary operator with respect to the generalized delta function.

Consider an operator A corresponding to the diffeomorphism f which is defined as $A|x\rangle = |f(x)\rangle$. Note that, x is the member of manifold M and also f is a function such that $f : M \rightarrow M$. From definition of A , we conclude that $\langle x | A^\dagger | y \rangle = \delta(f(x), y)$. By defining z through $z = f(x)$ we can get

$$\begin{aligned} \zeta(z) &= g(z) d^n z = g(z) \left| \det \left(\frac{\partial z}{\partial x} \right) \right| d^n x \\ &= \left(\frac{g \circ f}{g} \right) (x) |\det[(D(f)(x))]| \zeta(x) \end{aligned} \quad (24)$$

Now we can write

$$\zeta[f(x)] = \left(\frac{f^* g}{g} \right) (x) \zeta(x) \quad (25)$$

where f^* is the pullback of f and we have

$$(f^* g)_{\mu\nu}(x) = \left\{ g_{\alpha\beta}[f(x)] \right\} \frac{\partial f^\alpha}{\partial x^\mu} \frac{\partial f^\beta}{\partial x^\nu} \quad (26)$$

Using the equation (25), we find the following expression

$$\begin{aligned} \int \zeta(x) \delta(f(x), y) h(x) &= \int \zeta(z) (f^{-1}(z)) \delta(z, y) h(f^{-1}(z)) \\ &= \left(\frac{g}{f^* g} \right) (f^{-1}(y)) h(f^{-1}(y)) \end{aligned} \quad (27)$$

Note that, since f is a diffeomorphism so it is invertible. Therefore, f and its inverse are both differentiable. The equation (27) gives following equation

$$\delta(f(x), y) = \delta(x, f^{-1}(y)) \left(\frac{g}{f^* g} \right) (f^{-1}(y)) \quad (28)$$

Therefore,

$$\langle x | A^\dagger | y \rangle = \langle x | f^{-1}(y) \rangle \left(\frac{g}{f^* g} \right) (f^{-1}(y)) \quad (29)$$

Now we can extract the following equation from the above equation

$$A^\dagger | y \rangle = | f^{-1}(y) \rangle \left(\frac{g}{f^* g} \right) (f^{-1}(y)) \quad (30)$$

Note that, the equation (30) can be introduced as a universal formula for adjoint of the arbitrary linear operator.

5. Conclusion

Our investigation shows that a review of the fundamental properties of the delta function in generalized space. This subject seems to have received less attention independently in the research's papers. We have investigated the Heisenberg canonical relation only by using completeness relation in generalized space. In fact, it is impossible to derive the canonical relation without introducing the momentum operator properly, unless we use the special property of the delta function in generalized space. With the help of the equation (16), it is possible to discuss the Ehrenfest theorem in generalized space. We can see this in ref. [31], for a specific representation of the momentum operator in generalized space but they did not use the

generalized delta function at all. According to equation (30) we can obtain adjoint of every arbitrary linear operator. As a matter of fact, we have no restrictions in initial definition of $A|x\rangle = |f(x)\rangle$, for the form of the function $f(x)$ and in any case we can compute adjoint of A .

References

- [1] P. A. M. Dirac, *The principle of quantum mechanics*, 4th edition, Clarendon Press, Oxford, (1958).
- [2] J. D. Jackson, *Examples of the zeroth theorem of the history of science*, Am. J. Phys. **76**, (8), (2008).
- [3] A. Gangopadhyaya, C. Rasinariu, *Building confidence in the Dirac δ -function*, Eur. J. Phys. **39**, 6, 065402 (2018).
- [4] M. Belloni and R. W. Robinett, *The infinite well and Dirac delta function potentials as pedagogical, mathematical and physical models in quantum mechanics*, Physics Reports, **540**, 2 (2014).
- [5] A. G. Ushveridze, *Analytic properties of energy levels in models with delta-function potentials*, J. Phys. A: Math. Gen, **21**, (1988) 955-970.
- [6] C. K. Chua, Y. T. Liu and G. G. Wong, *Time-independent Green's function of a quantum simple harmonic oscillator system and solutions with additional generic delta-function potentials*,
- [7] S. H. Patil and, A. S. Roy, *Two-center double delta-function potential in one dimension*, Physica A **253**, (1998) 517-529.
- [8] P. Pedram, M. Vahabi, *Exact solutions of a Particle in a box with a delta function potential: The factorization method*, Am. J. Phys. **78**(8), (2010).
- [9] S. L. Nyeo, *Regularization methods for delta-function potential in two-dimensional quantum mechanics*, Am. J. Phys. **68**(6) (2000).
- [10] R. F. Hoskins, *Delta functions, Introductions to generalized functions*, 2ed, Woodhead Publishing (2011).
- [11] D. Griffiths and S. Walborn, *Dirac deltas and discontinuous functions*, Am. J. Phys. **67** (5), (1999).
- [12] Yu. V. Egorov, *A contribution to the theory of generalized functions*, Russian. Math. Surveys, 45:5, (1990) 1-49.
- [13] C.K. Raju, *Products and compositions with Dirac delta function*, J.Phys.A:Math.Gen.15, (1982) 381-396.
- [14] G. B. Arfken and H. J. Weber (2001), *Mathematical Methods for Physicists* 5th Ed. (Harcourt).
- [15] C. C. Barros Jr, *Quantum mechanics in generalized space-time*, Eur. Phys. J.C 42, 119-126(2005).
- [16] L. Viola and R. Onofrio, *Testing the equivalence principle through freely falling quantum Objects*, **55**, 2, (1997).
- [17] J. F. Doonoghue and B. R. Holstein, *Quantum mechanics in generalized space*, Am. J. Phys. 54(9), (1986).
- [18] Y. Q. Cai and G. Papini, *The effect of space-time curvature on Hilbert space*, General relativity and Gravitation, **22**, 3, (1990).
- [19] A. Karamatskou, H. Klinert, *Geometrization of the Schrodinger equation: Application of the Maupertuis principle to quantum mechanics*, Int.J.Geom.Methods.Phys.**11**, 8, (2014).

-
- [20] B. S .DeWitt, T. Stanev; *Point transformation in Quantum mechanics*, Phys. Rev. **85**, 653(1952).
- [21] P. D. Robinson and J. O. Hirschfelder, *Generalized momentum operators in quantum mechanics*, J. Math. Phys, **4**, 338(1963).
- [22] Gary R. Gruber, *Equivalence of Momentum Operators in Generalized Coordinates*, Am. J. Phys. **40**, 1702 (1972).
- [23] B. Leaf, *Momentum operators for curvilinear coordinate systems*, Am. J. Phys. **47**, 9 (1979).
- [24] Pedro. V-Gonzalez and Joel. C-Parra, *Quantum Operators in Generalized Coordinates*, Am. J. Phys. **49**, 8 (1981).
- [25] Youbang ZHAN, *On the momentum Operators and correspondence rule in curvilinear Coordinates in quantum mechanics*, Phys. Letters A. **128**, 9 (1988).
- [26] ChengShing Wang, *Generalized Coordinate representation in quantum mechanics*, Am. J. Phys. **57**, 1 (1989).
- [27] M. Carreau, *Momentum-space representation in generalized space*, Phys. Rev. D. **40**, 6 (1989).
- [28] M. Jafari Matehkolae, *Representation of the inverse momentum operator in generalized space*, Pramana -J. Phys. **93**:84 (2019).
- [29] D. I. Bonder, R. R. Lompay and Wing-Ki Liu; *Quantum mechanics of a free particle from properties of the Dirac delta function*, Am. J. Phys. **79**, 4 (2011).
- [30] M. Jafari Matehkolae, *Introducing the general condition for an operator in generalized space to be unitary*, 10.1088/1674-1056/abe300 (2020).
- [31] R.N. Costa Filho et al, *Extended uncertainty from first principles*, Phys .Lett B, 755, (2016) 367-370.
-

Solutions for simple quantum mechanical systems using SCILAB

Pankaj A. Nagpure

Department of Physics
Shri Shivaji Science College, Amravati
Amravati 444603, India.

nagpurepa@yahoo.co.in

Submitted on 07-10-2020

Abstract

The use of computer as a medium of learning has been proven can attract interest and motivation of students to study physics specially quantum mechanics. The Scilab as an open source computational software package provides various tools to simulate and solve the problems in quantum mechanics. In this paper the solution of Schrodinger equations are obtained for basic quantum mechanical systems like particle in infinite potential well, linear harmonic oscillator and hydrogen atom under various potential energy conditions imposed on the systems.

Scilab is the software for numerical computations and scientific visualization. It is capable of interactive calculations as well as automation of computations through programming. Its ability to plot 2D and 3D graphs helps in visualizing the data we work with. All these make Scilab an excellent tool for teaching, especially those subjects like quantum mechanics that involve matrix operations and solving of differential equations. Scilab can help the students to understand all the intermediate steps in solving even complicated problems, as easily as using a calculator. The greatest feature of Scilab is that it is free and it is available for many operating systems including Windows, Linux and MacOS X.

1. Introduction

A good use of the mathematics by teacher as a language in physics in the classroom is very important. If a teacher can demonstrate the solution of the complex physical problems graphically at different conditions, in real time with the classroom lesson took his or her teaching at higher level [1]. The programming in Scilab can be well used for the purpose [2].

In this paper solution of Schrodinger equations (Eigen values and Eigen functions) for some basic quantum mechanical systems at different potential conditions are obtained using Scilab software. The programs written in Scilab can be effectively used in the teaching and inspiring the students to explore various aspects of the systems discussed.

In the program, the build in function *ode* is used to solve the Schrodinger equations. The *if else* statement is used to get correct eigen value and corresponding eigen function which satisfy the given boundary conditions. The eigen functions are plotted in the graphics window of Scilab by using *plot* or *plot2d* function [3,4].

The two energy guesses (upper and lower) have to be provided through the *Scilab Console* after the execution of the program. The energy guesses are such that one of the guess energy values leads to the positive value and another leads to negative value of wave function at the boundary.

2. Basic quantum mechanical systems

The Schrodinger equations for following quantum mechanical systems [5] are solved for eigen values of energies and corresponding eigen functions.

- i. Particle in infinite square well potential
- ii. Linear harmonic oscillator
- iii. Hydrogen atom

i. Particle in infinite square well potential

If $\psi(x)$ be the wave function for particle then the Schrodinger time independent wave equation for a particle is,

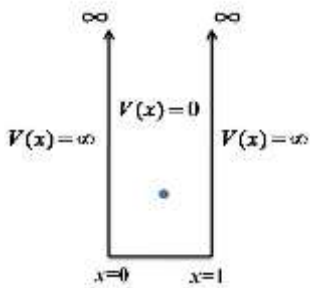
$$\frac{d^2\psi}{dx^2} + \frac{2m}{\hbar^2}(E - V(x))\psi = 0$$

Here we take an electron as a particle in infinite square well. For an electron $mc^2 = 0.511 \times 10^6 \text{ eV}$, width of the well $a = 1 \text{ \AA}$ and a constant, $\hbar c = 1973 \text{ eV \AA}$. The symbol u is used instead of ψ for wave function in the program. The above Schrodinger equation is solved for following potential energy conditions.

A. $V(x)=0$ for $0 < x < 1$

$$V(x)=\infty \text{ for } x \leq 0 \therefore \text{ for } x \leq 0, \quad \psi(x)=0$$

$$V(x)=\infty \text{ for } x \geq 1 \therefore \text{ for } x \geq 1, \quad \psi(x)=0$$



$$\therefore \frac{d^2\psi}{dx^2} + \frac{2mE}{\hbar^2}\psi = 0, \text{ for } 0 < x < 1$$

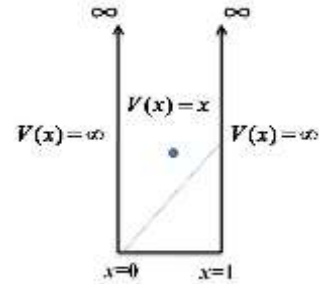
Energy eigen values and eigen functions are given by

$$E_n = \frac{n^2 \pi^2 \hbar^2 c^2}{2mc^2 a^2} \text{ and } \psi_n = \sqrt{\frac{2}{a}} \sin \frac{n\pi x}{a}.$$

B. $V(x)=x$ for $0 < x < 1$

$$V(x)=\infty \text{ for } x \leq 0 \therefore \text{ for } x \leq 0, \quad \psi(x)=0$$

$$V(x)=\infty \text{ for } x \geq 1 \therefore \text{ for } x \geq 1, \quad \psi(x)=0$$

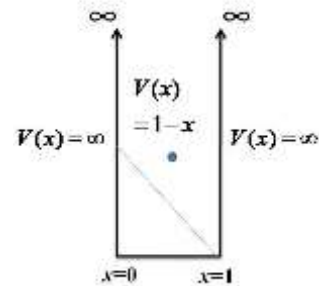


$$\therefore \frac{d^2\psi}{dx^2} + \frac{2m}{\hbar^2}(E - x)\psi = 0, \text{ for } 0 < x < 1$$

C. $V(x)=1 - x$ for $0 < x < 1$

$$V(x)=\infty \text{ for } x \leq 0 \therefore \text{ for } x \leq 0, \quad \psi(x)=0$$

$$V(x)=\infty \text{ for } x \geq 1 \therefore \text{ for } x \geq 1, \quad \psi(x)=0$$

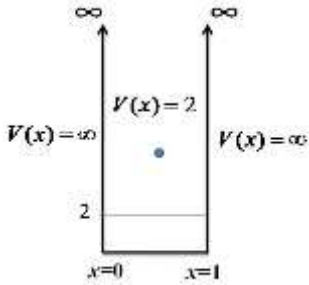


$$\therefore \frac{d^2\psi}{dx^2} + \frac{2m}{\hbar^2}(E - (1 - x))\psi = 0, \text{ for } 0 < x < 1$$

D. $V(x)=2$ for $0 < x < 1$

$$V(x)=\infty \text{ for } x \leq 0 \therefore \text{ for } x \leq 0, \quad \psi(x)=0$$

$$V(x)=\infty \text{ for } x \geq 1 \therefore \text{ for } x \geq 1, \quad \psi(x)=0$$

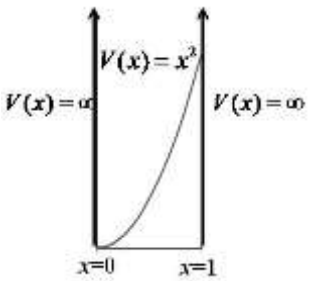


$$\therefore \frac{d^2\psi}{dx^2} + \frac{2m}{\hbar^2}(E - 2)\psi = 0, \text{ for } 0 < x < 1$$

E. $V(x) = x^2$ for $0 < x < 1$

$V(x) = \infty$ for $x \leq 0 \therefore$ for $x \leq 0, \psi(x) = 0$

$V(x) = \infty$ for $x \geq 1 \therefore$ for $x \geq 1, \psi(x) = 0$

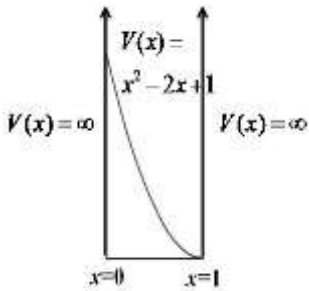


$$\therefore \frac{d^2\psi}{dx^2} + \frac{2m}{\hbar^2}(E - x^2)\psi = 0, \text{ for } 0 < x < 1$$

F. $V(x) = x^2 - 2x + 1$ for $0 < x < 1$

$V(x) = \infty$ for $x \leq 0 \therefore$ for $x \leq 0, \psi(x) = 0$

$V(x) = \infty$ for $x \geq 1 \therefore$ for $x \geq 1, \psi(x) = 0$

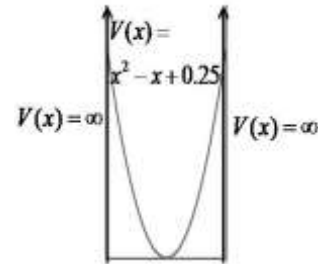


$$\therefore \frac{d^2\psi}{dx^2} + \frac{2m}{\hbar^2}(E - (x^2 - 2x + 1))\psi = 0, \text{ for } 0 < x < 1$$

G. $V(x) = x^2 - x + 0.25$ for $0 < x < 1$

$V(x) = \infty$ for $x \leq 0 \therefore$ for $x \leq 0, \psi(x) = 0$

$V(x) = \infty$ for $x \geq 1 \therefore$ for $x \geq 1, \psi(x) = 0$



$$\therefore \frac{d^2\psi}{dx^2} + \frac{2m}{\hbar^2}(E - (x^2 - x + 0.25))\psi = 0, \text{ for } 0 < x < 1$$

```

1 //Infinite square well potential problem
2 clc;clf;
3 function du=f(x,t,E);
4 ... m=0.511*10^6;h=1973;
5 ... V=(x^2-x+0.25)
6 ... du(1)=t(2);
7 ... du(2)=- (2*m/(h*h)) * (E-V) *t(1);
8 endfunction
9 E1=input("Enter the value first guess of energy=")
10 E2=input("Enter the value second guess of energy=")
11 x0=0;u0=0;u0p=1;
12 for i=1:100
13 ... x=0:0.001:1;
14 u1=ode([u0;u0p],x0,x,list(f,E1))
15 u2=ode([u0;u0p],x0,x,list(f,E2))
16 E3=(E1+E2)/2
17 u3=ode([u0;u0p],x0,x,list(f,E3))
18 if(u1(1,1001)*u3(1,1001))<0;
19 ... then
20 ... E2=E3;
21 else
22 ... E1=E3;
23 end
24 end
25 disp('Energy eigen value=');
26 disp(E3);
27 plot2d(x,u3(1,:))
    
```

Figure 1: Scinote (Infinite Square Well)

Table 1: Energy eigen values at different potential energies inside the well

n	E_n (eV) using formula	E_n (eV) using Scilab program for potential energies inside the well discussed in above cases						
	$V(x)=0,$ $0 < x < 1$	A	B	C	D	E	F	G
1	37.6229	37.59265	38.09236	38.09236	39.59265	37.87503	37.87503	37.62532
2	150.491	150.3706	150.8707	150.8707	152.3706	150.6913	150.6913	150.4413
3	338.606	338.3339	338.8339	338.8339	340.3339	338.6616	338.6616	338.41163
4	601.966	601.4825	601.9825	601.9825	603.4825	601.8127	601.8127	601.56271
5	940.573	939.8164	940.3164	940.3164	941.8164	940.1478	940.1478	939.89778
6	1354.42	1353.335	1353.835	1353.835	1355.335	1353.667	1353.667	1353.4177
7	1843.52	1842.040	1842.540	1842.540	1844.040	1842.372	1842.372	1842.1226
8	2407.86	2405.930	2406.430	2406.430	2407.930	2406.262	2406.262	2406.0127
9	3047.45	3045.005	3045.505	3045.505	3047.005	3045.338	3045.338	3045.0882
10	3762.29	3759.265	3759.766	3759.766	3761.265	3759.598	3759.598	3759.3487

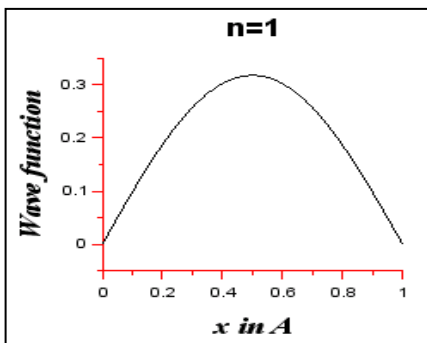


Figure 2:a. Ground State (n=1) Eigen Function

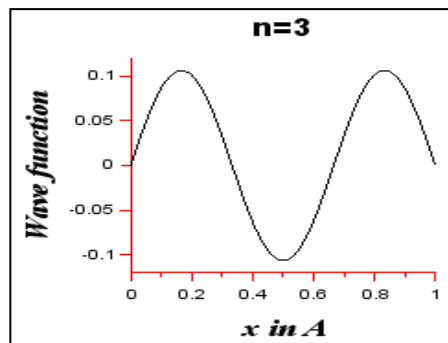


Figure 4:C. Second Excited State (n=3) Eigen Function

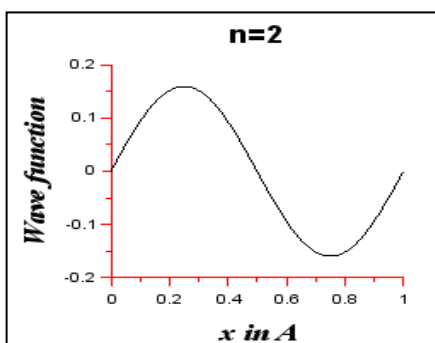


Figure 3:b. First Excited State (n=2) Eigen Function

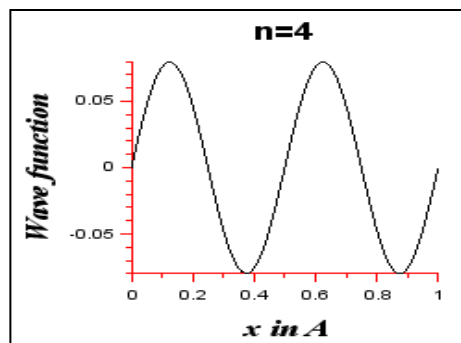


Figure 5:d. Third Excited State (n=4) Eigen Function

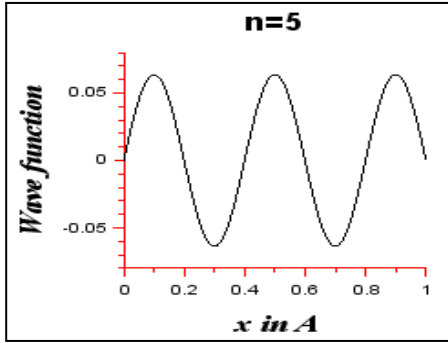


Figure 6:e. Fourth Excited State (n=5) Eigen Function

ii. Linear harmonic oscillator

Here we take a particle in linear harmonic oscillator potential $V(x)$. For a particle $mc^2 = 940$ MeV and a constant, $\hbar c = 197.3$ eV nm. If $\psi(x)$ be the wave function for particle then the Schrodinger time independent wave equation for a particle is,

$$\frac{d^2\psi}{dx^2} + \frac{2m}{\hbar^2}(E - V(x))\psi = 0$$

Energy eigen values and eigen functions are given by

$$E_n = (n + \frac{1}{2})\hbar c \sqrt{\frac{k}{mc^2}}$$

$$\psi_n(x) = \frac{1}{\sqrt{\sqrt{\pi} 2^n n! x_0}} e^{-x^2/2x_0^2} H_n\left(\frac{x}{x_0}\right), \quad \text{where}$$

$$x_0 = \sqrt{\frac{\hbar}{\sqrt{km}}}$$

The above Schrodinger equation is solved for following potential energy conditions.

A. $V(x) = \frac{1}{2} kx^2$ (take force constant $k=100$)

$$\frac{d^2\psi}{dx^2} + \frac{2m}{\hbar^2}\left(E - \frac{1}{2}kx^2\right)\psi = 0$$

B. $V(x) = \frac{1}{2} kx^2 + bx$ (take force constant $k=100$)

and anharmonicity constant $b=10$)

C. $V(x) = \frac{1}{2} kx^2 + bx^2$ (take force constant $k=100$ and anharmonicity constant $b=10$)

D. $V(x) = \frac{1}{2} kx^2 + bx^3$ (take force constant $k=100$ and anharmonicity constant $b=10$)

```

1 //Harmonic oscillator potential problem
2 clear;clc;clf
3 function du=f(r,t,E,b);
4     m=940;h=197.3;
5     V=(100*(r^2))/2+(b*r^3)
6     du(1)=t(2);
7     du(2)=(2*m/(h*h))*(V-E)*t(1);
8 endfunction
9 b=input("Anharmonicity constant (b)=")
10 E1=input("Enter the value first guess of energy=")
11 E2=input("Enter the value second guess of energy=")
12 r0=0;u0=0;u0p=1;
13 acc=abs(E1-E2);
14 while acc>0.0000001
15     acc=abs(E1-E2)
16     r=0:0.01:20;
17 u1=ode([u0;u0p],r0,r,list(f,E1,b))
18 u2=ode([u0;u0p],r0,r,list(f,E2,b))
19 E3=(E1+E2)/2
20 u3=ode([u0;u0p],r0,r,list(f,E3,b))
21 if (u1(1,2001)*u3(1,2001))<0;
22     then
23         E2=E3;
24 else
25         E1=E3;
26 end
27 end
28 disp(E3);
29 plot(r,(u3(1,:))^2,"linewidth",5)
    
```

Figure 7: Scinote (Harmonic Oscillator)

Table 2: Energy eigen values of harmonic oscillator at different potential energies

N	E_n (eV) using formula	E_n (eV) using Scilab program for potential energies of HO discussed in above cases			
	$E_n = (n + \frac{1}{2})\hbar c \sqrt{\frac{k}{mc^2}}$	A	B	C	D
0	32.17608				
1	96.52825	96.52825	105.4735	105.7414	106.8960
2	160.8804				
3	225.2326	225.2326	238.7132	246.7299	260.0095
4	289.5847				
5	353.9369	353.9369	370.8137	387.7185	420.1967
6	418.2891				
7	482.6412	482.6412	502.3473	528.707	585.5672
8	546.9934				
9	611.3456	611.3456	633.527	669.6955	755.1367

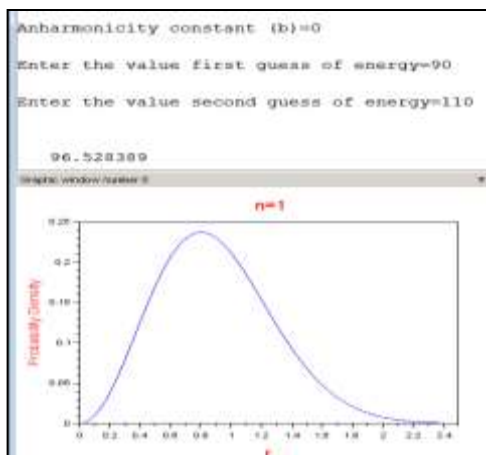


Figure 8: Probability density plot for n=1

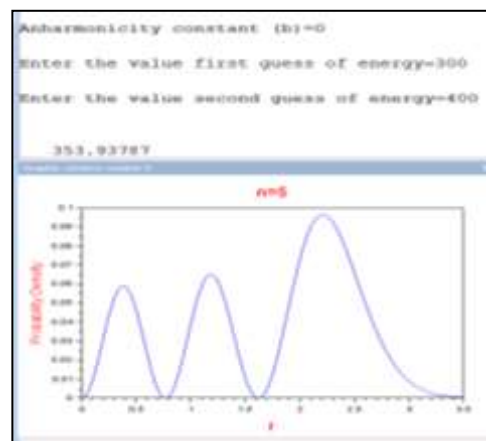


Figure 10: Probability density plot for n=5

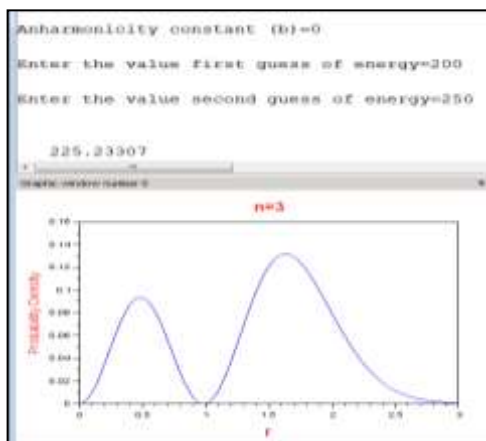


Figure 9: Probability density plot for n=3

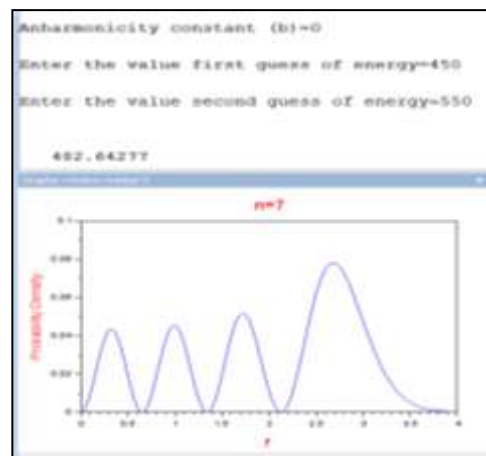


Figure 11: Probability density plot for n=7

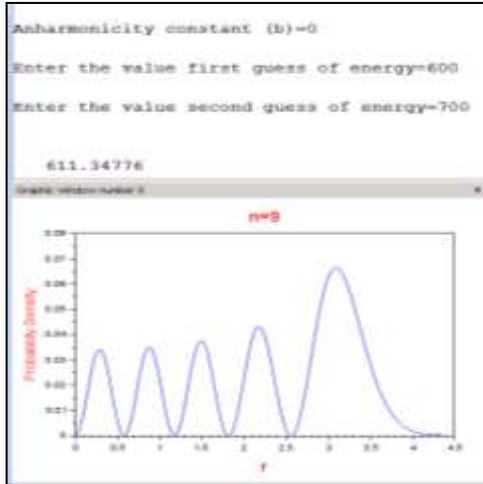


Figure 12: Probability density plot for n=9

iii. Hydrogen atom

The hydrogen atom is the simplest example for an atomic system consists of nucleus (a proton) and an orbiting electron. If $\psi(r, \theta, \phi)$ be the wave function for this two particles system, then the Schrodinger time independent wave equation for the system will be,

$$-\frac{\hbar^2}{2\mu} \nabla^2 \psi(r, \theta, \phi) + V(r)\psi(r, \theta, \phi) = E\psi(r, \theta, \phi)$$

Where, $V(r) = \frac{-e^2}{4\pi\epsilon_0 r}$ is the potential energy and

$$\mu = \frac{mM}{m+M} \approx m \text{ is the reduced mass of the system}$$

and

$$\nabla^2 = \frac{1}{r^2} \frac{\partial}{\partial r} \left(r^2 \frac{\partial}{\partial r} \right) + \frac{1}{r^2 \sin \theta} \frac{\partial}{\partial \theta} \left(\sin \theta \frac{\partial}{\partial \theta} \right) + \frac{1}{r^2 \sin^2 \theta} \frac{\partial^2}{\partial \phi^2}$$

The Schrodinger equation can be separated into radial and angular wave equations. Here only the radial wave equation is solved, since it gives the eigen values of energies.

$$\frac{1}{r^2} \frac{d}{dr} \left(r^2 \frac{dR_l}{dr} \right) + \left[\frac{2\mu E}{\hbar^2} - \frac{2\mu V}{\hbar^2} - \frac{l(l+1)}{r^2} \right] R_l = 0$$

$$R_l(r) = \frac{u(r)}{r} \Rightarrow$$

$$\frac{d^2 u}{dr^2} + \left[\frac{2\mu E}{\hbar^2} - \frac{2\mu V}{\hbar^2} - \frac{l(l+1)}{r^2} \right] u = 0$$

For electron

$$e = 3.795, mc^2 = 0.511 \times 10^6 \text{ eV and } \hbar c = 1973 \text{ eV \AA}^0$$

The constant factor $\frac{1}{4\pi\epsilon_0}$ is included in above value

of e . $l=0,1,2,3,\dots$ is orbital quantum number. For ground state, only one value of l (i.e. $l=0$) is allowed, for first excited two values of l (i.e. $l=0, 1$) are allowed and so on.

Energy eigen values and eigen functions are given

$$\text{by } E_n = -\frac{\mu e^4}{2\hbar^2 n^2} = -\frac{e^2}{2a_0 n^2} = -\frac{13.6}{n^2} \text{ eV, } a_0 = \frac{\hbar^2}{\mu e^2}$$

and

$$R_{nl} = -\left(\frac{2}{na_0}\right)^{3/2} \sqrt{\frac{(n-l-1)!}{2n[(n+l)!]^3}} \left(\frac{2r}{na_0}\right)^l e^{-r/na_0} L_{n+l}^{2l+1} \left(\frac{2r}{na_0}\right)$$

```

1 //hydrogen atom
2 clc;clf
3 function du=f(r,t,E,l);
4     e=3.795;m=0.511*10^6;h=1973;
5     du(1)=t(2);
6     du(2)=(2*m/(h*h))*(-(e*e)/r)-E)*t(1)+(1*(1+1)*r^(-2))*t(1);
7 endfunction
8 E1=input("Enter the value first guess of energy=")
9 E2=input("Enter the value second guess of energy=")
10 l=input("Orbital quantum number (l)=")
11 r0=0.01;u0=0.01;u0p=1;
12 for i=1:50
13     r=0.01:0.01:20;
14 u1=ode([u0;u0p],r0,r,list(E,E1,l))
15 u2=ode([u0;u0p],r0,r,list(E,E2,l))
16 E3=(E1+E2)/2
17 u3=ode([u0;u0p],r0,r,list(E,E3,l))
18 if(u1(1,2000)*u3(1,2000))<0;
19     then
20         E2=E3;
21 else
22         E1=E3;
23 end
24 end
25 disp(E3);
26 plot(r,(u3(1,:))^2,"linewidth",10);
27 replot([0 3;0 0.05])
28

```

Figure 13: Scinote (H-atom)

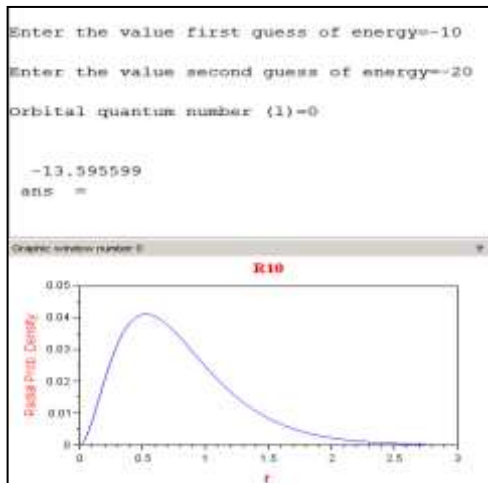


Figure 14: a. Energy Eigen Value and Radial Wave Function for $n=1$ and $l=0$

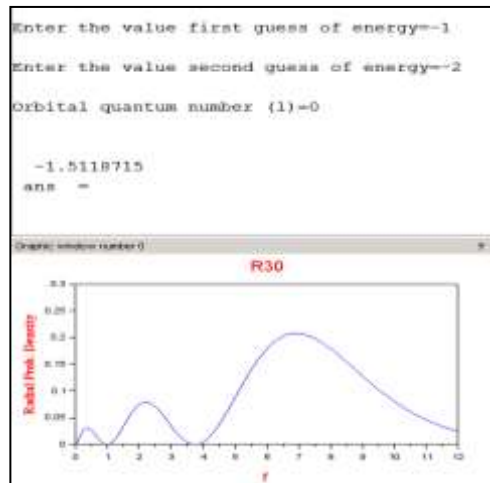


Figure 17: d. Energy Eigen Value and Radial Wave Function for $n=3$ and $l=0$

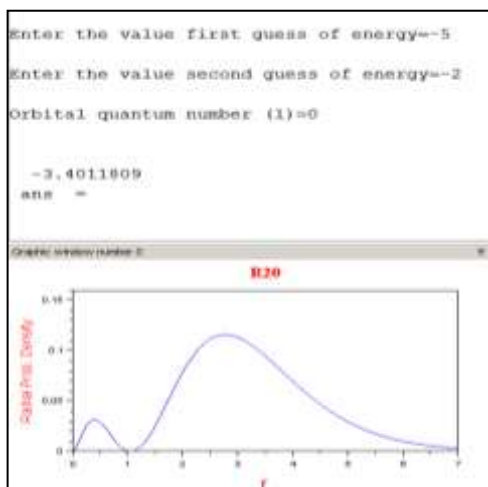


Figure 15: b. Energy Eigen Value and Radial Wave Function for $n=2$ and $l=0$

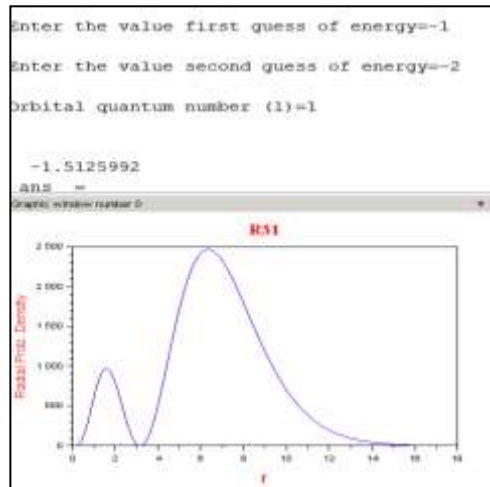


Figure 18: e. Radial Wave Function for $n=3$ and $l=1$

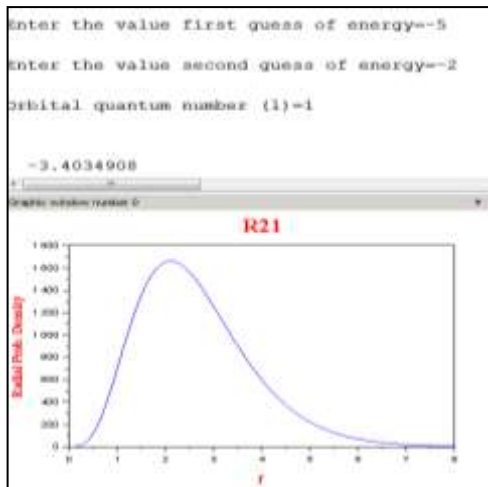


Figure 16: c. Energy Eigen Value and Radial Wave Function for $n=2$ and $l=1$

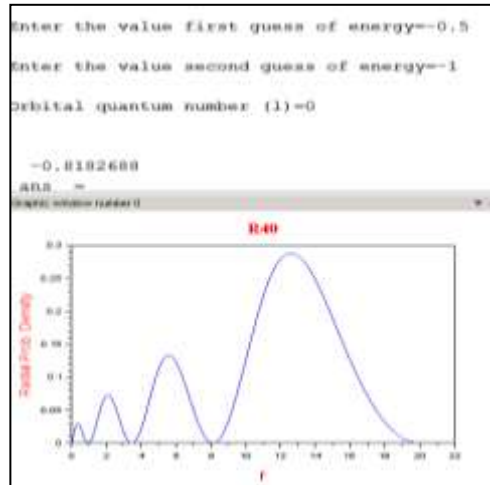


Figure 19: f. Radial Wave Function for $n=4$ and $l=0$

3. Conclusions

The present work is comprehensive illustration of nature of solutions of Schrodinger equations and eigen values of energies of quantum mechanical systems taught at undergraduate level. These programs can be effectively used in the classroom teaching to explore different aspects of the quantum mechanical systems.

4. References

[1] Jack M. Wilson and Edward F. Redish, Using Computers in Teaching Physics,

Physics Today, January 1989, 34-41.

[2] SCILAB Version 6.0.0, <http://www.scilab.org/>

[3] Scilab for very beginners, Scilab Enterprises, 2013.

[4] Scilab Textbook Companion for Quantum Physics Of Atoms, Molecules, Solids, Nuclei And Particles by Eisberg And R. Resnick (2019)

[5] Nouredine Zettili, *Quantum Mechanics: Concepts and Applications* (John Wiley & Sons, Inc. 2009)

A simple model of electric ground and of a dc power supply

Carl E. Mungan

Physics Department, U.S. Naval Academy, Annapolis, MD 21402 USA

mungan@usna.edu

Submitted on 16-03-2021

Abstract

In a direct-current (dc) circuit, a power supply and a ground can each be modeled as a large, distant, conducting sphere bearing a net surface charge. The relation between the charge on and potential of each of these spheres is analyzed before and after they are connected to a concentric spherical capacitor that is initially uncharged. Expressions for the potential at all points in the vicinity of the charged capacitor (both inside and outside it) are written down.

Students are frequently confused about the relationship between the charge on and potential of a grounded surface or of the terminals of a dc power supply. The following problem can help illustrate some of the key concepts. A solid metal sphere of radius $R_1 = 1$ cm is surrounded by a concentric spherical metal shell of inner radius $R_2 = 5$ cm and small radial thickness. Thin wires are connected to the shell and sphere (by passing through a small hole in the shell in

order to reach the central sphere). One wire is used to ground the inner sphere, and another to connect the shell to an emf of $\xi = 5$ V. Find the potential at a point P that is 6 cm from the center of the sphere. The geometry is shown in Fig. 1.

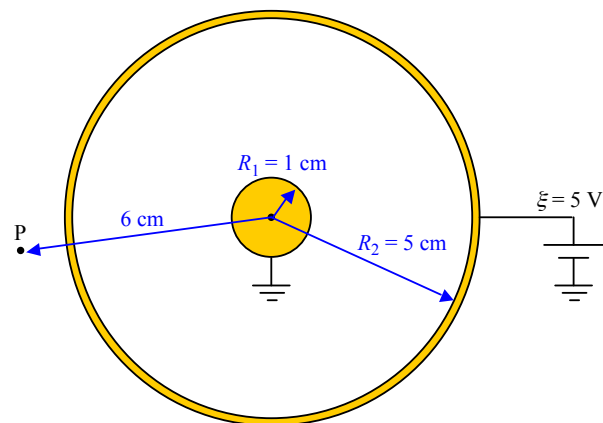


Figure 1: A grounded 1-cm-radius metal sphere surrounded by a concentric metal shell connected to the positive terminal of a 5 V dc power supply. (That implies the power supply cannot be floating but must have its negative terminal grounded.) Find the potential at point P just outside the shell.

To solve this problem, students should recognize that “ground” is a big conductor (like the Earth) which defines the reference potential of 0 V. Model it here as a metal sphere of radius R large compared to R_1 and R_2 . Students often believe zero potential implies zero charge, but that is not true in general. In fact, the surface of the Earth has a net negative charge relative to the atmosphere [1]. To be general, suppose the large grounded sphere has charge Q_0 on its surface.

Likewise, the 5 V supply can be modeled as another metal sphere of the same large radius R . These two large spheres must be located far away from both the concentric system (of the shell and inner sphere) and each other, so that they do not interact electrically with them. Thus the two connection wires must be long. To be specific, suppose they are straight with one pointing radially north and the other radially east away from the center of the 1-cm sphere, as sketched in Fig. 2. One of the large spheres has a potential of 5 V relative to the other, grounded sphere; the separation distance between them is so large (compared to all radii in the problem) that it can be approximated as infinite. Thus the charge Q_5 on the sphere of potential $\zeta = 5$ V must be greater than that on the grounded sphere such that

$$\frac{kQ_5}{R} - \frac{kQ_0}{R} = \zeta \quad (1)$$

where k is the Coulomb constant.

To be exact, Q_5 and Q_0 are the charges on the two large spheres when switches S_1

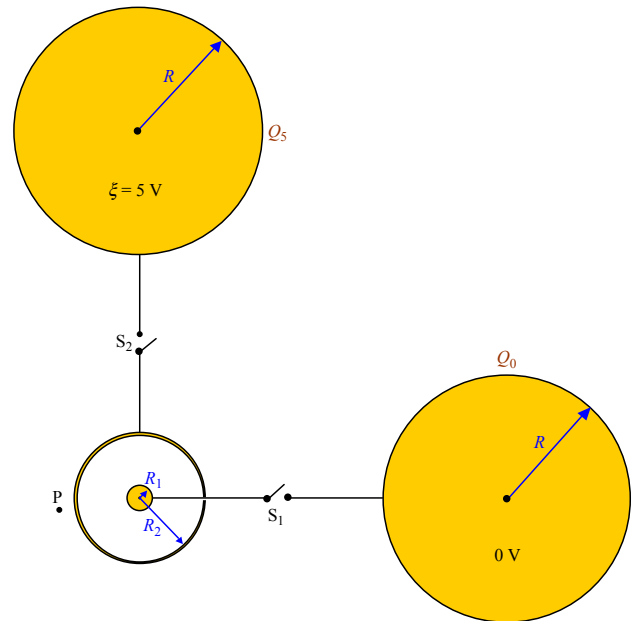


Figure 2: Ground is modeled as a metal sphere of large radius R connected via a long wire through switch S_1 to the inner sphere of radius R_1 . The potential ζ is sourced by a metal sphere of the same large radius R connected via another long wire through switch S_2 to the outer shell of radius R_2 . (The figure is not to scale: the length of the two wires and radius R of the two large spheres are actually much bigger.) With both switches initially open, there are charges Q_5 and Q_0 on the large spheres, whereas the concentric spherical capacitor is uncharged.

and S_2 in Fig. 2 are open. Now close both switches. Some charge must flow along the two wires to set the potential of the central small sphere to 0 V (since it is connected to the reference large sphere) and the potential of the concentric shell around it equal to that of the supply large sphere which ends up being ΔV that is slightly smaller than 5 V. To achieve electrostatic equilibrium, positive charge Q must flow onto the shell and

migrate entirely to its inner surface, where it will distribute itself uniformly. The same amount of charge must flow off the central sphere to ground, leaving it with a net charge of $-Q$ uniformly distributed on its surface, as depicted in Fig. 3. (The usual assumption is made that there is negligible charge on the two long wires assuming they are thin enough [2].) This charge distribution guarantees there is no electric field within the metal composing either the central sphere or the concentric shell (i.e., in the gold-shaded regions of Fig. 1) as must be true for conductors in equilibrium. All electric field lines that start on the inner surface of the shell terminate on the surface of the central sphere.

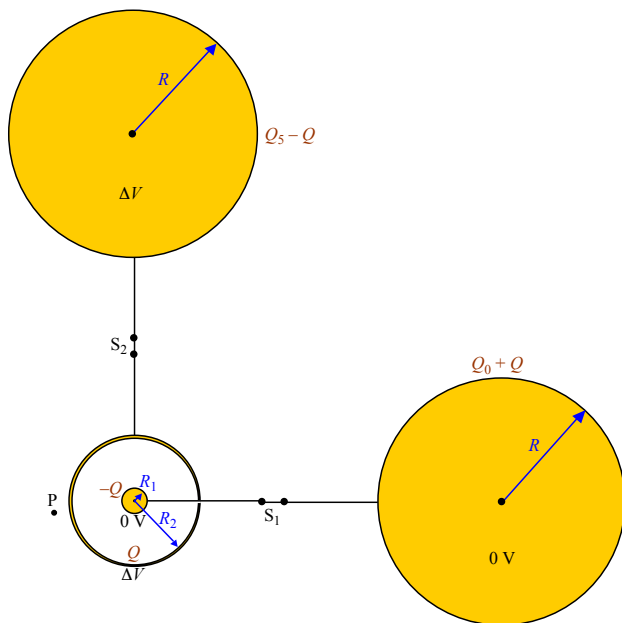


Figure 3: Charges on and potentials of the four spherical conductors after switches S_1 and S_2 are closed and electrostatic equilibrium is established.

Meanwhile the large spheres are so far away that their electric fields are negligible near this concentric capacitor. Thus there is no electric field between the outer surface of the shell and the point P that is 1 cm away from it. Consequently there is no potential difference between the shell and that point, and thus the potential at point P is ΔV which will be negligibly different than 5 V for spheres of radius R large enough to serve as an ideal ground and power supply.

Students may have performed the common laboratory experiment of mapping out the equipotential curves for a pair of concentric cylinders in a water tray [3] or drawn with silver paint on conductive paper [4]. In that case, they may remember that the potential everywhere inside the inner cylinder is equal to the value on its surface, and likewise the potential everywhere outside the outer cylinder is equal to the value on its surface. Those experimental observations corroborate the theoretical results presented above.

To carry the analysis one step further, how does the exact potential difference ΔV between the concentric shell of radius $R_2 = 5$ cm and the inner sphere of radius $R_1 = 1$ cm depend on the value of R in Fig. 3? The answer is that ΔV is a bit smaller than $\xi = 5$ V owing to the flow of charge Q along the wires, as follows.

The charge on the grounded sphere ends up being $Q_0 + Q$. Nevertheless it remains the reference and thus its potential is still 0 V by definition. It is connected by a

wire to the central sphere having charge $-Q$ on it. Thus the potential on that inner sphere must also be 0 V, and so the potential in the space between it and the surrounding shell is

$$V(r) = -\frac{kQ}{r} + \frac{kQ}{R_1} \quad (2)$$

for any radial distance r from the center of the sphere in the range $R_1 \leq r \leq R_2$. Specifically $V(R_2)$ is equal to

$$\Delta V = -\frac{kQ}{R_2} + \frac{kQ}{R_1}. \quad (3)$$

Meanwhile, the charge on the large supply sphere equilibrates to $Q_5 - Q$. Thus the potential difference between it and the grounded sphere is

$$\frac{k(Q_5 - Q)}{R} - \frac{k(Q_0 + Q)}{R} = \Delta V. \quad (4)$$

Substituting Eq. (1) into the left-hand side of Eq. (4) gives

$$\xi - 2\frac{kQ}{R} = \Delta V. \quad (5)$$

Finally, eliminating Q between Eqs. (3) and (5) results in

$$\Delta V = \frac{R_2 - R_1}{R_2 - R_1 + 2R_1R_2/R} \xi. \quad (6)$$

For example, if $R_1 = 10$ mm, $R_2 = 50$ mm, and $R = 1000$ mm then Eq. (6) becomes

$$\Delta V = \frac{40}{41}(5 \text{ V}) \approx 4.88 \text{ V} \quad (7)$$

which is 2.4% smaller than 5 V. On the other hand, if the two large spheres are ten times

larger in radius (i.e., $R = 10$ m) then Eq. (6) gives

$$\Delta V = \frac{400}{401}(5 \text{ V}) \approx 4.988 \text{ V}. \quad (8)$$

One sees that ΔV can be made as close to 5 V as one likes, by choosing the grounded and supply conductors big enough. This result illustrates that any large conductor can serve as a source or sink of charge while its potential remains nearly constant.

In summary, an initially uncharged spherical capacitor receives equal and opposite charges $\pm Q$ on its facing surfaces when one of its conductors is connected to ground and the other to a dc power supply of emf ξ . By modeling that ground and power supply as large, distant metal spheres, the relationship between the charge on and potential of each of them is clarified, which can help improve student understanding of these concepts. In particular, the larger in radius those distant spheres are, the smaller will be the drop in the potential difference between them when they are connected to the spherical capacitor. Furthermore, the potential in the vicinity of the capacitor varies only in the space between their facing surfaces, and is constant inside the inner sphere and outside the outer spherical shell composing it.

References

- [1] R. Feynman, R.B. Leighton, and M.L. Sands, *The Feynman Lectures on Physics*

- (Addison-Wesley, Reading MA, 1964)
Vol. II, Chap. 9.
- [2] G.-P. Tong, "Electric charge on the wire connecting two spheres," *Am. J. Phys.* **62**, 709–712 (Aug. 1994).
- [3] R.B. Khaparde and H.C. Pradhan, "An experiment on equipotential curves," *Phys. Edu.* **27**, 27–38 (Jan.–Mar. 2010).
- [4] D.O. Ludwigsen and G.N. Hassold, "A simple electric field probe in a Gauss's law laboratory," *Phys. Teach.* **44**, 470–472 (Oct. 2006).

Realizing Positive Temperature Co-efficient of Resistance Effect using an IC-555 Timer Circuit

K. M. Anand¹, J. Mukherjee² and K. Prasad²

¹Department of Electronics and Communication Engineering
S.R.M. Institute of Science and Technology
Chennai 603203, India.

²University Department of Physics
T.M. Bhagalpur University
Bhagalpur 812007, India.

prasad_k@tmbuniv.ac.in

Submitted on 26-07-2020

Abstract

In this paper, a simple yet effective and alternative method is described to observe the temperature dependence of resistance of a positive temperature coefficient of resistance (PTCR) by making use of a free-running multivibrator constructed around IC-555 Timer. Since the output pulse width of a free-running multivibrator is a function of the capacitances and the resistances attached to the circuit, this property along with the fact that resistance varies with the temperature to which the component is subjected can be exploited to study the variation of resistance along with the temperature. The width of the output pulse and resistance was found to increase with the rise in temperature. Hence, the circuit could be utilized for temperature sensing applications. Furthermore, this method may also be used to determine the value of an unknown resistance $R(T)$ attached to the circuit and the value of the temperature coefficient

of resistance (α). This simple and cost-effective method could be included as an experiment in the curriculum of various undergraduate and/or post-graduate courses and can also be taken upon as a project work by interested students.

1. Introduction

Many engineering applications often require a positive temperature coefficient (PTC) materials. Such materials show an increase in electrical resistance upon raising their temperature. They are being used especially in PTC temperature sensors and PTC thermistors as they display linear characteristics. Besides, resistances, a basic electrical component find its uses in our everyday life. Whether simple electronic gadgets or complex machines such as televisions and satellites, these components are used everywhere and are one of the most widespread electrical components. Resistance as the word signifies is basically opposed to the flow of electric current in the circuit. Naturally, a curious mind would ask if the resistance

offered by the aforementioned is of a fixed value or does it depend on some external factors. As known, the resistivity increases with increasing temperature in conductors and vice versa. Further, the multivibrator can be constructed utilizing BJTs or by employing a versatile IC-555 timer in the free-running (astable) mode on a logic breadboard. With the intent to examine the variation of resistance with temperature, especially the PTCR effect, a free-running multivibrator has been constructed around IC-555 timer with the sample heating arrangement. The development of such a simple experiment will surely offer an undergraduate (UG) and/or post-graduate (PG) student a better apprehension of the issue and would produce an involvement in natural philosophy (science) in particular [1-3]. Accordingly, in the present work, a method is discussed to study the temperature dependence of resistance (PTCR effect) with the help of an IC-555 timer circuit in astable mode connection by correlating them with the output pulse width. Also, the generated temperature-dependent output pulses width has been verified using *PSpice*[®] electronic simulation software.

2. Relevant Theory

The resistance of a PTC component such as that of a simple resistor is a function of temperature to which it is subjected. The higher the temperature, it is subjected to, the higher is the resistance offered by it. The absolute value of the resistance at a particular temperature is given by the equation:

$$R(T) = R_{ref} \{1 + \alpha(T - T_{ref})\} \quad (1)$$

Here R_{ref} is the resistance at some reference temperature T_{ref} , α is the temperature coefficient of resistance of the material used and T_{ref} is some reference temperature at which α is specified assuming that the length and area don't change with temperature. Besides, the output pulse width ($W \equiv W_{on}$; during ON time) of IC-555 timer in astable mode at pin no. 3 (fig. 1) is given as [5]:

$$W = 0.693(R_A + R_B)C \quad (2)$$

The terms R_A , R_B , and C are the resistances and capacitance as indicated in fig. 1. As is evident from the above equations, the time period of the output pulse is a function of R_A , R_B , and C . If any of these values are altered, the output pulse width will change accordingly. Further, with an aim to protect the circuit, a resistance (R_S) was connected in series with $R(T)$ and hence the value of $R_A = R(T) + R_S$.

Therefore, eqn. (2) can be rewritten as

$$W = 0.693\{R(T) + R_S + R_B\}C \quad (3)$$

It is clear from eqn.(3) that if the values of R_B and C kept constant, the value of R_A i.e. $R(T)$ controls the width of output pulse (W). Thereby, knowing the experimental value of W , one can very easily estimate the value of $R(T)$ at any particular temperature and consequently its variation with temperature. We have from eqns. (1) and (3),

$$W = 0.693\{R_S + R_{ref}(1 + \alpha\Delta T) + R_B\}C \quad (4)$$

Here, the change in temperature, $\Delta T = T - T_{ref}$. It is noticed from this expression that W is directly proportional to ΔT . Hence, using the experimental value of T or ΔT in eqn. (3), W can be easily being calculated. Hence, using expressions (3) and (4) the temperature dependence of resistance can be obtained using Timer-555 operating in astable mode.

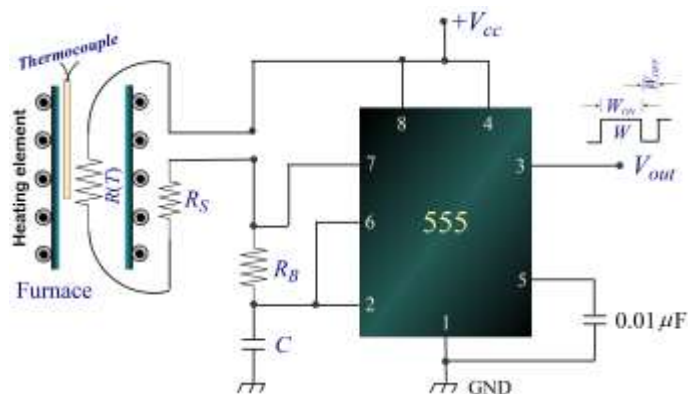


FIG. 1: External connection diagram to realize the PTCR effect using IC-555 timer in astable mode with sample heating arrangement.

3. Experimental Detail

3.1. Circuit Diagram

Fig. 1 shows the external connection diagram of IC-555 timer for astable mode operation with sample heating arrangement. A heater coil of 1500 watt is used as the sample resistance $R(T)$. The value of $R(T) = 37\Omega$ at room temperature (27°C) was taken in the present study. As stated earlier, to protect the circuit a series resistance $R_S = 300\Omega$ has been connected with $R(T)$ so that value of $R_A = R(T) + R_S$. However, the interested reader may change the value by changing the materials as well as the length of the wire to see the effect on the output pulse width. The entire circuit is built-up around IC-555 timer on a logic breadboard. The output pulse width can be seen and measured on a CRO screen connected across pin number 3.

3.2. Design considerations

Theoretically, there is not any sort of restrictions on the values of R_A , R_B and C however depending upon the least count of the oscilloscope, the scale of the oscilloscope used and the resistance of the coil (present case) at the room temperature there is a need to restrict the values of R_A , R_B , and C in order to observe significant changes in the width of the pulse produced by the free-running multivibrator. In this experiment, the value of R_A was taken as 337Ω at room temperature. Further, it is known that if the value of $R_B \gg R_A$ then there would hardly be any difference in the time period of the output pulse and the very purpose of the experiment would stand defeated. Accordingly, the value of R_B was chosen as $1.5\text{k}\Omega$ so that any change in the coil's resistance with a change in temperature would show a significant difference in the CRO. Also, the value of the capacitance, C was chosen as $1\mu\text{F}$ for the same reason.

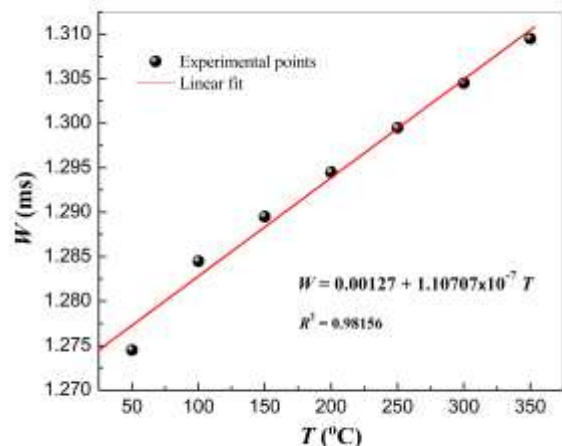


FIG. 2: Variation of experimentally observed output pulse width (W) with temperature.

4. Results and Discussion

Fig. 2 shows the variation of output pulse width (W) at pin 3 with temperature along with the fitted curve. It is noticed that the width of the output pulse increases with the rise in T . A linear least-squares fitting of W - T data yielded the equation $W = 0.0012 + 1.10707 \times 10^{-7} T$ with the adjusted $R^2 = 0.98156$.

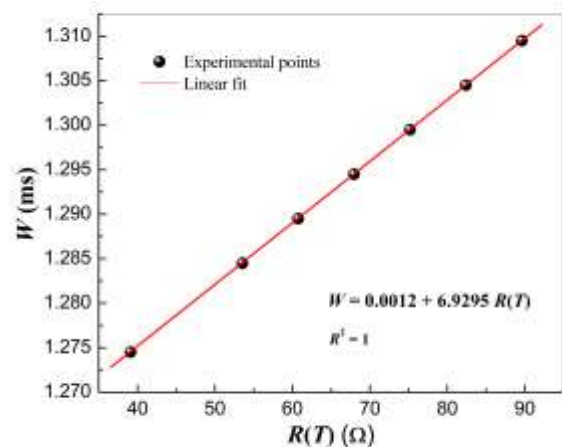


FIG. 3: Variation of resistance $R(T)$ with output pulse width (W) as a calibration curve.

The values of $R(T)$ at different temperatures were obtained from the eqn. (3) using the experimentally observed values of W and were plotted as a calibration curve (Fig. 3). A linear regression analysis of the W - $R(T)$ data gives rise to the equation:

$$W = A + B.R(T) \tag{5}$$

The value of coefficients was estimated to be $A = 0.0012$ and $B = 6.9295$ and the value of the regression coefficient (R^2) between eqn. (5) and the experimental data was found to be 1. Therefore, any experimentally measured value W could be substituted in eqn. (5) and consequently, the corresponding value of resistance can easily be obtained at a given temperature. The value of $R(T)$ may also be estimated graphically from the calibration curve (Fig.3).

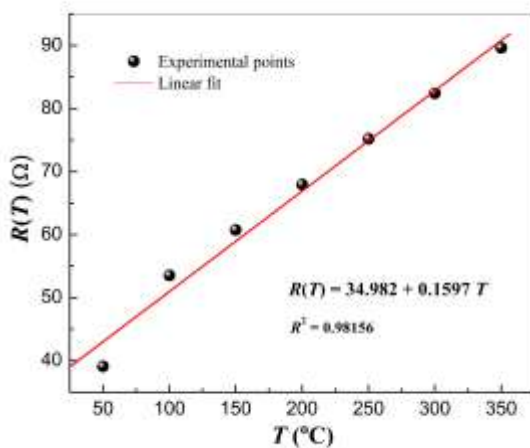


FIG. 4: Temperature variation of resistance $R(T)$ showing PTCR effect.

The temperature variation of resistance has been presented in Fig. 4. It is seen that the value of resistance increases with the rise in temperature *i.e.* the system shows the linear temperature-dependent resistance response in the present range of investigation, which indicates the positive temperature coefficient of resistance (PTCR) behavior. Such a behavior could be understood as the electrons flowing through a conductor (heater

element, present case) are being impeded by atoms with the rise in temperature, and the number of phonons gets increased *i.e.* The atoms start vibrating with higher amplitude. These vibrations in turn cause frequent collisions between the free electrons and the other electrons. Each collision drains out little energy of the free electrons which restrict their movement (delocalized electrons). This, in turn, restricts the current flow in the sample and consequently led to an increase in resistance or resistivity of the material with the increase in temperature. A line of best fit was obtained as $R(T) = 34.982 + 0.1597 T$ with the adjusted $R^2 = 0.98156$. The value of the temperature coefficient of resistance of the sample at room temperature was estimated to be 0.00432 ($^{\circ}\text{C}$) $^{-1}$ using the relation: $\alpha = R_{ref}^{-1} \cdot dR(T) / dT$. The positive value of α also supported the PTCR behavior of the test sample.

These observations were verified by the *PSPice*[®] electronic simulation software. Figs. 5(a) and 5(b), respectively display the output pulses for $R(50^{\circ}\text{C}) = 39.11\Omega$ and $R(350^{\circ}\text{C}) = 89.61\Omega$. It is noticed that the values of W are nearly comparable to the experimental results. Also, noticed that the output pulse width (W_{off}) remains constant during the OFF time of IC-555 timer in the astable mode for every temperature. This is because the discharge path contains R_B and C only as $W_{off} = 0.693R_B C$ [5].

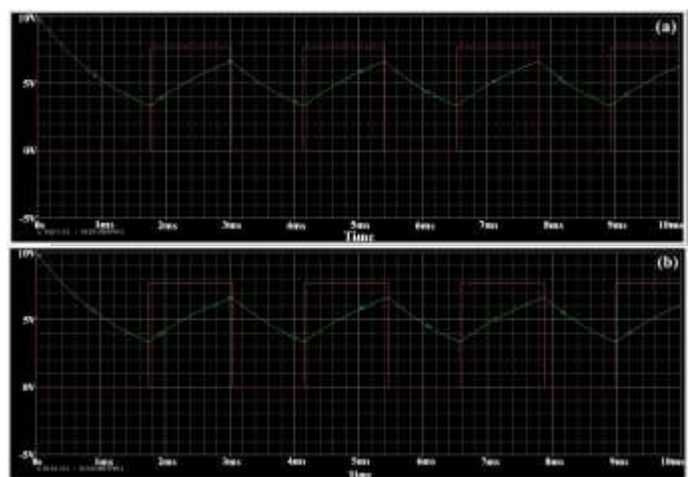


FIG. 5: Output pulses when (a) $R_{50^{\circ}\text{C}} = 39.11\Omega$ and (b) $R_{350^{\circ}\text{C}} = 89.61\Omega$ as observed in *PSPice*[®] electronic simulation software.

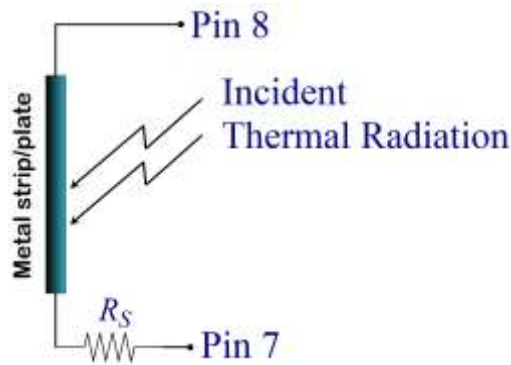


FIG. 6: Schematic diagram of temperature sensing device.

It is to note that the value of R_S will rely upon the specimen used as $R(T)$. Hence, this technique may either be used to know the value of unknown resistance at a particular temperature as well as their dependence, $R(T)$ on T . Furthermore, since $W \propto R(T)$ and consequently $W \propto T$, the present circuit could easily be extended as a temperature sensor. The schematic diagram of the same is presented in Fig. 6.

5. Conclusions

The experiment performed in this article enabled us to get an insight into and/or provide an alternative method to study the temperature variation of the resistance of a PTCR material. With little alteration and a bit of intuitive thinking, this experiment can be

extended to study the coefficient of thermal expansion and could also be used to obtain the resistivity ($\rho = RA/l$) of a material. Apart from this, the variation of resistance of a negative temperature coefficient (NTC) component such as that of a diode could also be studied by replacing the resistance coil with a diode connected in reverse biased mode and consequently the bandgap of the semiconductor. Such a cost-effective experiment can easily be arranged in any UG and/or PG laboratory which will help the students to develop scientific insight, scientific temper, and inculcate an interest in the field of research. Also, one may use other materials like ceramics, ceramic/polymer composites, nanomaterials, *etc.* for intended applications. Thus, it is recommended as project work for those who are interested in physics, electronics, electrical technology, and material science.

References :

- [1] S.S. Verma, K. Prasad, N.P. Singh, T.K.S.P. Gupta, *Ind. J. Tech. Edu.* **19**, 43–45 (1996).
- [2] K. Prasad, N. Nath, K. Prasad, *Ind. J. Phys.* **74A**, 387–389 (2000).
- [3] K. Prasad, *Phys. Edu.* **18**, 37–41 (2001).
- [4] Subrato, K.M. Anand, Archana Kumar, and K. Prasad, *AIP Conf. Proc.* **2220**, 040007-4 (2020).
- [5] D. Roy Choudhury, and S.B. Jain, *Linear Integrated Circuits*, (New Age Int. Publ., New Delhi, 4th Edn., 2014).